HEAT TRANSPORT BY RESIDUAL GASES IN MULTILAYER VACUUM INSULATION

R. S. Mikhal'chenko, A. G. Gerzhin, V. T. Arkhipov, N. P. Pershin, and L. V. Klipach

Inzhenerno-Fizicheskii Zhurnal, Vol. 14, No. 1, pp. 148–155, 1968

UDC 536.2:621.52

The results of an experimental investigation of residual gas heat-transfer in multilayer vacuum insulation are reported. The "thermal paradox" observed when the cold-wall temperature changes from 77 to 20.4° K is explained. Graphs of the variation of the residual gas pressure in the insulation layers are given and the components of the total heat flux—radiative and residual gas—are determined.

In studying the thermal conductivity of multilayer vacuum insulation on the calorimetric apparatus described in [1] we observed a decrease in heat flow by

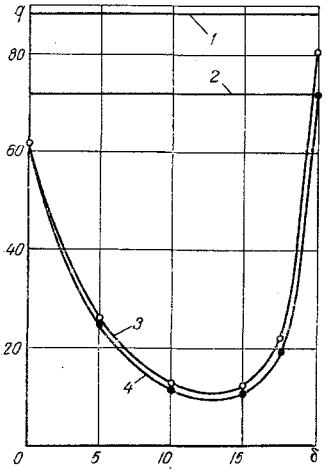

Fig. 1. Variation of total specific heat flux and its components over the thickness of the specimen: 1 and 2) total specific heat flux; 3 and 4) radiative specific heat flux (boundary temperatures 300–77° K for 1 and 3; 300–20.4° K for 2 and 4).

15–20% when the temperature of the cold wall changed from 77 to 20.4° K at constant hot wall temperature. The decrease in heat flow for 10–15 liter vessels was 30–35% under the same conditions. This "thermal paradox" has also been observed by other authors [2–5] in various types of insulation.

In multilayer insulation heat transfer depends on radiation, conduction through the solid material, and on the thermal conductivity of the residual gas. Most authors disregard the residual gas, i.e., assume that $\lambda = f(T)$. Then the specific heat flux through an insulation package of thickness δ with boundary temperatures T_1 and T_2 can be written as

$$q_1 = -\frac{1}{\delta}\int_{T_1}^{T_2} \lambda\, dT. \qquad (1)$$

When the cold wall temperature falls from T_2 to T_3,

$$q_2 = -\frac{1}{\delta}\int_{T_1}^{T_3} \lambda\, dT = -\left[\frac{1}{\delta}\int_{T_1}^{T_2} \lambda\, dT + \frac{1}{\delta}\int_{T_2}^{T_3} \lambda\, dT\right],$$

i.e.,

$$q_2 = -\left[q_1 + \frac{1}{\delta}\int_{T_2}^{T_3} \lambda\, dT\right]. \qquad (2)$$

It follows from (2) that the observed decrease in heat flux with fall in the cold wall temperature cannot be attributed to a decrease in the emissivity of the surfaces and an increase in the thermal resistance of the contacts with decreasing temperature, as assumed in [2].

Consequently, there must be a factor that affects the heat transmission through the insulation but does not depend on the temperature. This factor may be the residual gas pressure in the layers of insulation. A similar suggestion was made in [5].

Our object was to study the effect of the residual gas pressure on the heat transfer in multilayer vacuum insulation.

From the kinetic theory of gases, for the low-pressure region, when the condition $Kn = L/d \gg 1$ is satisfied, the molecular heat-transfer due to the residual gas enclosed between two parallel surfaces at temperatures T_1 and T_2 is given by [6]

$$q_g = 1.82 \cdot 10^3 \frac{\gamma+1}{\gamma-1}\, a_0\, \frac{T_1 - T_2}{\sqrt{MT}}\, P\ \mu W/cm^2 \qquad (3)$$

where T is the temperature of the medium surrounding the manometer.

The freely stacked insulation package investigated consisted of reflecting sheets (screens) separated by fine fibrous packing of porosity m = 0.9. The distance between sheets was 0.36 mm. For nitrogen the minimum L/d ratio is 3.1 at an interval pressure of 5.3 N/m^2 and a temperature of 246° K and for hydrogen it is 16 at 1.86 N/m^2 and 210° K. Assuming that the gas molecules move freely through the packing without colliding with the individual fibers, we can use Eq. (3) to study the residual gas heat transfer in the pressure range $1.33–1.33 \cdot 10^{-4}$ N/m^2. To find the pressure in the layers of insulation we developed a method which reduced to the experimental determination of q, T_1, T_2, and a. The other quantities were taken from published sources.

Experimental method. We used the flat calorimeter described in [1] with a specimen of annealed aluminum

sheets 14 μ thick separated by SBR-M glass paper 40 μ thick with elementary fibers 5–7 μ in diameter. The specimen was 20 mm thick, and the stacking density was 28 sheets/cm. Edge effects were eliminated with a plastic foam protector ring, with a temperature distribution similar to that in the specimens. The temperature in the specimen and at the protector ring was measured with precalibrated copper-constantan thermocouples. We used a R-306 potentiometer and an M17/2 galvanometer. The maximum error in the temperature did not exceed ±0.2°. Before being inserted in the specimen each thermocouple was bonded to the protector ring over 250 mm at a level with a temperature close to that in the specimen. This almost eliminated the parasitic heat flow along the thermocouples Six thermocouples were used: two on sheets 1 and 56, the rest between sheets 14 and 15, 28 and 29, 42 and 43, and 49 and 50. The temperatures of these sheets were determined graphically.

The pressure in the calorimeter cavity was measured in the range $1.33 \cdot 10^{-5}$–$1.33 \cdot 10^{-1}$ N/m^2 with two LM-2 ionization gauges and in the range $1.33 \cdot 10^{-1}$–13.3 N/m^2 with two LT-2 thermocouple gauges in combination with VIT-1A vacuum gauges. The rated total pressure measuring error is not greater than ±15% for the LM-2 gauges and ±30% for the LT-2 gauges. However, since the experimental gauge readings did not differ by more than 5% in the former case and 10% in the latter, the total pressure measuring error can be considered better than the instrument ratings.

The heat flow was assumed to be steady when the gas flow rate and the temperature of the aluminum sheets became constant. The total error in measuring the heat flux was less than ±5%.

Experimental results. To determine the residual gas pressure in the layers of insulation we used Eq. (3) in the form

$$P = 5.5 \cdot 10^{-4} \frac{\gamma - 1}{\gamma + 1} \frac{\sqrt{MT}}{T_n - T_{n+1}} \frac{q_g}{a_0}. \quad (4)$$

In analyzing the experimental data we made the following assumptions:

a) the pressure between the cold wall of the calorimeter and the adjacent aluminum sheet was taken equal to the pressure in the calorimeter; this assumption is based on the fact that for screen and separation-layer temperatures below 125° K, their gas separation is very small, while the gas remaining between them is evaluated by the cold wall.

b) the heat transfer by solid conduction is less than 10% [7, 8] and can be neglected. Accordingly, strictly speaking, the data obtained below (Figs. 1, 3, and 4) are not absolute, but make it possible to estimate the nature of the relations and typical values of the components of the specific heat flux and of the gas pressure in the layers of insulation.

With these assumptions we write

$$q_g = q_t - q_r, \quad (5)$$

where q_t was determined experimentally at variable pressure in the calorimeter cavity and q_r stems from

$$q_r = \varepsilon_{red} \sigma (T_n^4 - T_{n+1}^4), \quad (6)$$

where ε_{red} is the reduced emissivity as a function of temperature of two aluminum sheets separated by a

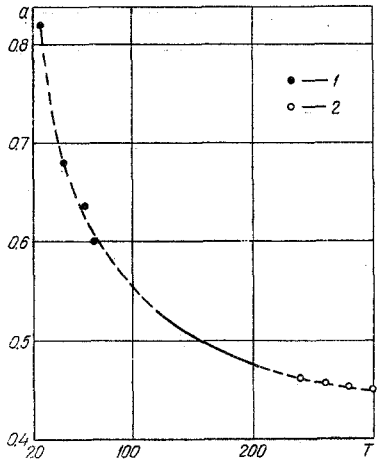

Fig. 2. Accommodation factor of hydrogen as a function of temperature: 1) experimental data computed from Eqs. (5) and (6); 2) computed from Eq. (8).

layer of glass paper. The value of ε_{red} was determined from other experiments and on the temperature interval 300–77° K varied linearly from 0.02 to 0.031. It should be noticed that the reduced emissivity of the aluminum sheets without glass insulation had approximately the same values. This means that in first approximation the glass-fiber material is largely transparent to infrared radiation in the region 10–54 μ.

The variation of q_g over the thickness of the specimen is shown in Fig. 1 for the boundary temperatures 300–77 and 300–20° K and a vacuum of $4 \cdot 10^{-5}$ N/m^2 in the calorimeter (in Figs. 1, 3, and 4 the abscissas are reckoned from the hot wall).

The quantity a_0 in Eq. (4) given in terms of the accommodation factor is

$$a_0 = \frac{a}{2 - a}. \quad (7)$$

Preliminary calculations on the experimental data showed that the accommodation factor for gaseous nitrogen at the cold wall of the calorimeter lies in the range 0.89–0.92 on the pressure interval $6.5 \cdot 10^{-4}$–1.33 N/m^2. Our accommodation factors for nitrogen are in good agreement with the data of [9] for surfaces covered with unknown adsorbed gases. Consequently, in constructing the curves in Fig. 3 the variation of the accommodation factors with temperature for nitrogen as well as for air were taken from the data of [9]. When the pressure in the calorimeter cavity varied from $2.66 \cdot 10^{-5}$ to $2.66 \cdot 10^{-1}$ N/m^2, the accommodation factor for gaseous hydrogen at the cold wall varied from 0.588 to 0.82. The accommodation factor defined as a measure of the completeness of energy transfer in a collision, is by definition independent of the pressure. Its increase is apparently attributable to the fall in the

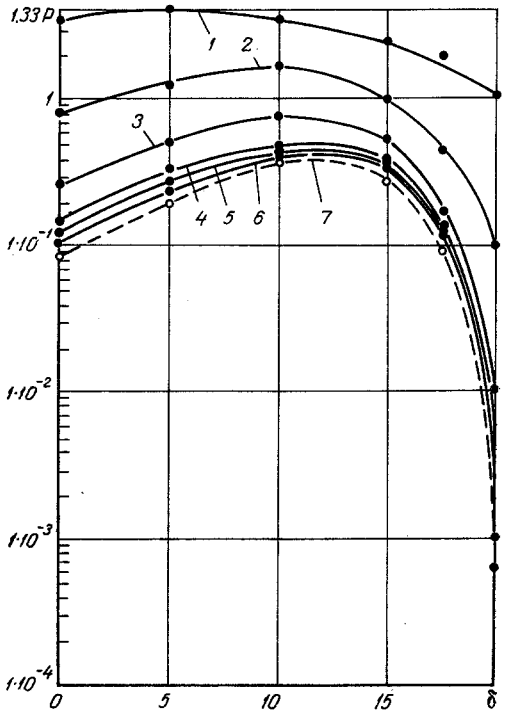

Fig. 3. Pressure in the layers of insulation as a function of the pressure in the calorimeter cavity for the boundary temperatures 300–77° K (filler gas nitrogen): 1) at calorimeter pressure of 1.33 N/m^2; 2) $1.33 \cdot 10^{-1}$; 3) $1.33 \cdot 10^{-2}$; 4) $1.33 \cdot 10^{-3}$; 5) $6.6 \cdot 10^{-4}$; 6) $4.2 \cdot 10^{-5}$; 7) $4 \cdot 10^{-5}$ for the boundary temperatures 300–20.4° K.

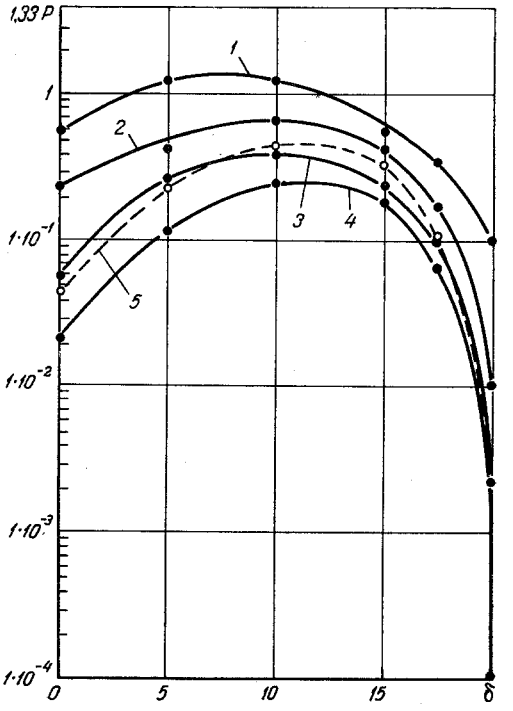

Fig. 4. Pressure in the layers of insulation as a function of the pressure in the calorimeter cavity for the boundary temperatures 300–20.4° K (1–4—filler gas hydrogen; 5—air): 1) at a calorimeter pressure of $1.33 \cdot 10^{-1}$ N/m^2; 2) $1.33 \cdot 10^{-2}$; 3) $2.33 \cdot 10^{-3}$; 4) $1.33 \cdot 10^{-4}$; 5) $1.33 \cdot 10^{-4}$.

Thermal Conductivities and Specific Heat Fluxes Obtained on a Flat Calorimeter and on a Dewar-Type Calorimeter

Apparatus	δ, mm	T_1, °K	T_2, °K	λ_{eff}, μW/cm·°K	q, μW/cm²	P_{calor}, N/m²
Flat calorimeter	20	300	77	0.778	86.9	$4.4 \cdot 10^{-5}$
			20.4	0.472	71.4	$3.5 \cdot 10^{-5}$
Dewar-type calorimeter	12	295	77	0.895	134.1	$9.3 \cdot 10^{-5}$
			20.4	0.43	80.5	$4.2 \cdot 10^{-5}$

temperature of the aluminum sheet from 124 to 32° K, which corresponds to the data of [10], and a possible increase in the contamination of the cold surface of the calorimeter with adsorbed gases as the pressure rises.

To determine the pressure in the specimen for hydrogen on the temperature interval 120–230° K (Fig. 4) we used the experimental data on the accommodation factors given by Rowley and Evans in [11], and presented as a straight line of $\ln(1/a - 1)$ versus 1/T. To facilitate the extrapolation of the temperature dependence of the accommodation factor the broad temperature range 300–30° K, we reduced the data of Rowley and Evans to a and T coordinates (Fig. 2), where the dashed line gives the extrapolated values of the accommodation factor. In the temperature interval 120–30° K extrapolation was carried out according to the character of the reduced curve. As seen from Fig. 2, the extrapolated values of the accommodation factors agree closely with our experimental values. The extrapolated values of the accommodation factors on the temperature interval 230–300° K were plotted based on the Yuskin-Bertram equation

$$\ln\left(\frac{1}{a} - 1\right) = \frac{Q - E_a}{RT} + \text{const}, \qquad (8)$$

which closely reproduces the experimental value the accommodation factor obtained by Rowley and Evans on the temperature inverval 120–230° K [11]. To find the extrapolated values of the accommodation factor we reduce Eq. (8) to the form

$$\frac{1}{a} - 1 = C + C\frac{Q - E_a}{RT}, \qquad (9)$$

where C = const.

In the expansion of the exponential in Eq. (8) we retain only first-degree terms. The difference $Q - E_a$ and the coefficient C for the temperature interval 220–300° K in Eq. (9) were taken equal to their values on the temperature interval 200–220° K, since on the interval in question the effect of the third term of the series is not important and the change in Q and E_a is only slight.

Figures 3 and 4 represent the pressure distribution in the layers of insulation as a function of the pressure in the calorimeter cavity for the boundary temperatures 300–77 and 300–20.4° K.

Curve 5 in Fig. 4 was constructed using the accommodation factor for air [9] at a calorimeter pressure of $1.33 \cdot 10^{-4}$ N/m². The actual pressure in the layers will lie between curves 4 and 5, since at this pressure it may be assumed that there is a mixture of hydrogen and residual gas between the layers.

From an examination of Figs. 1, 3, and 4 we may draw the following conlusions:

a) residual gas heat-transfer plays an important part in the total heat flow through multilayer vacuum insulation even at a vacuum of better than $1 \cdot 10^{-3}$ N/m² in the insulation cavity.

b) the residual pressure in the layers of insulation (Fig. 3, curve 6) at a calorimeter cold-wall temperature of 77° K exceeds the residual pressure (curve 7) in the case of a cold-wall temperature at 20.4° K for the same pressure in the calorimeter cavity, namely $4 \cdot 10^{-5}$ N/m². Thus, the reduced pressure in the second case offers a good explanation of the "thermal paradox."

c) the nonuniform pressure distribution over the thickness of the specimen, minimal in the layers adjacent to the walls of the calorimeter and maximal in the central zone, is explained not only by the reduction in vapor pressure with decrease in the temperature of the layers but also by the more favorable evacuation conditions when the temperature of the cold wall is reduced from 77 to 20.4° K.

In order to illustrate the "thermal paradox" we have tabulated the effective thermal conductivities and specific heat fluxes obtained on a flat calorimeter [1] and a ten-liter Dewar-type calorimeter for the given type of insulation.

NOTATION

a is the accommodation coefficient; q is the specific heat flux; q_t, q_r, q_g are the specific heat fluxes: total, radiative, and gas; λ is the thermal conductivity; T is the temperature, °K; T_n is the temperature of the n-th sheet; δ is the thickness of the specimen, mm; L is the molecular mean free path, mm; b is the distance between sheets, mm; Kn is the Knudsen number; P is the gas pressure, N/m²; $\sigma = 5.77 \cdot 10^{-12}$ W·cm^{-2}·deg^{-4} is the radiation constant; $\gamma = c_p/c_v$ is the ratio of specific heats; M is the molecular weight; Q is the heat of adsorption; E_a is the activation energy; and R is the universal gas constant.

REFERENCES

1. R. S. Mikhal'chenko, A. G. Gerzhin, and N. P. Pershin, IFZh [Journal of Engineering Physics], 11, no. 5, 1966.

2. R. H. Kropschot, J. E. Schrodt, M. M. Fulk, and B. J. Hunter, Advances in Cryogenic Engineering, 5, 189, 1960.

3. M. M. Fulk, Progress in Cryogenics, **1**, 65, 1959.

4. H. M. Strong, F. P. Bundy, and H. P. Bovenkerk, J. Appl. Phys., **31**, no. 1, 39, 1960.

5. I. A. Black and P. E. Glaser, Advances in Cryogenic Engineering, **6**, 32, 1961.

6. G. K. White, Experimental Techniques in Low-Temperature Physics [Russian translation], GIFML, Moscow, 213–214, 1961.

7. M. G. Kaganer, Thermal Insulation in Low-Temperature Technology [in Russian], izd. Mashinostroenie, Moscow, 1966.

8. J. D. Verschoor and P. Greebler, Transactions of ASME, **74**, no. 6, 961, 1952.

9. L. B. Thomas and F. G. Olmer, J. Am. Chem. Soc., **65**, 1036, 1943.

10. W. H. Keesom and G. Schmidt, Physica, **4**, 828, 1937.

11. M. Kaminsky, Atomic and Ionic Impact Phenomena on Metal Surfaces, 56–95, 1965.

1 January 1967

Physicotechnical Institute of Low Temperatures, Khar'kov